Supporting Information:

Undercooling-directed NaCl crystallization: an approach towards nanocavities-linked graphene network for fast lithium and sodium storage

Yaxin Chen,[1,2,4] Liluo Shi,[2,5] Da Li,[2] Yue Dong,[2] Qiong Yuan,[2] Shaozhuan Huang,[3] Hui Ying Yang,[3] Xianyong Wei,[4] Quanchao Zhuang,[1] Zhicheng Ju,[1]* Huaihe Song[2]*

[1] The Jiangsu Province Engineering Laboratory of High Efficient Energy Storage Technology and Equipments, School of Materials Science and Physics, China University of Mining and Technology, Xuzhou 221116, P. R. China.

[2] State Key Laboratory of Chemical Resource Engineering, Beijing Key Laboratory of Electrochemical Process and Technology for Materials, Beijing University of Chemical Technology, Beijing 100029, P. R. China.

[3] Pillar of Engineering Product Development, Singapore University of Technology and Design, 8 Somapah Road, Singapore 487372, Singapore.

[4] Key Laboratory of Coal Processing and Efficient Utilization (Ministry of Education), China University of Mining and Technology, Xuzhou 221116, China.

[5] College of Chemistry and Chemical Engineering, Xuzhou University of Technology, Xuzhou, 221111 China.

*Corresponding author E-mail: juzc@cumt.edu.cn.

songhh@mail.buct.edu.cn

Supplementary Figures

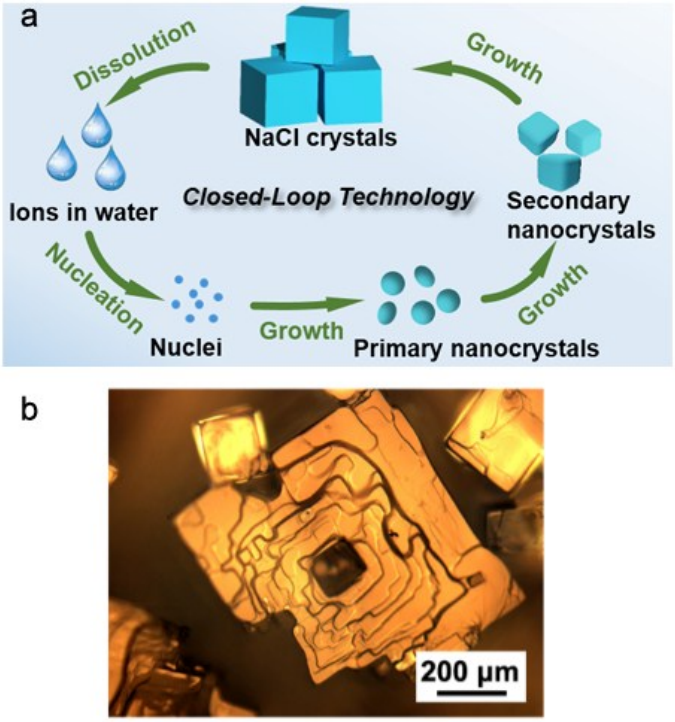

Fig. S1. (a) Schematic diagram of the closed-loop NaCl crystallization; (b) microscopy image of NaCl crystals grown at room temperature.

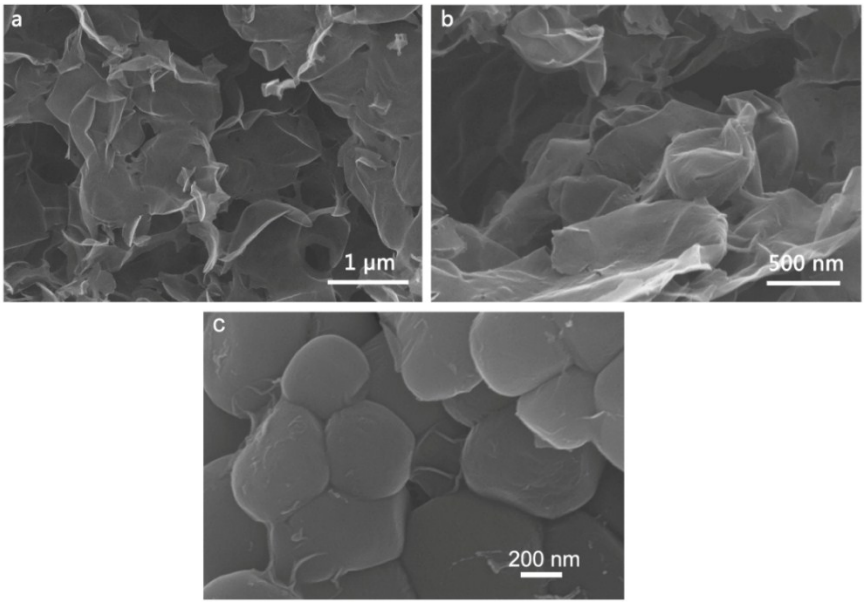

Fig. S2. SEM images of (a,b) CGN and (c) pre-CGN.

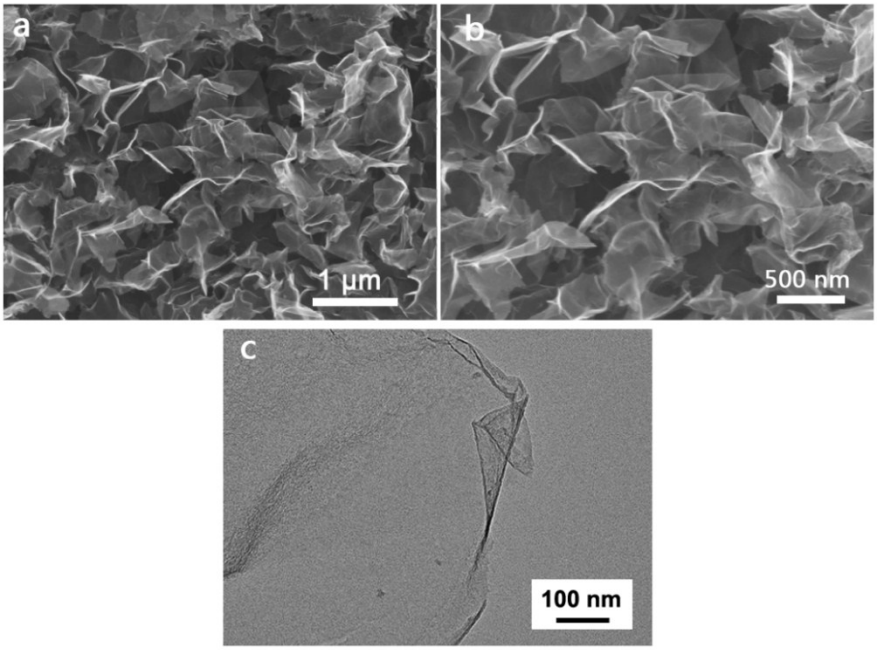

Fig. S3. (a,b) SEM and (c) TEM images of GNS

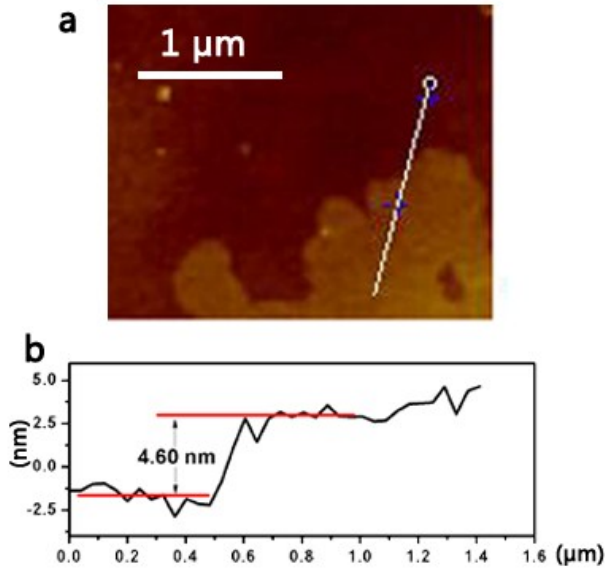

Fig. S4. AFM image of GNS with the corresponding height profile along the white path.

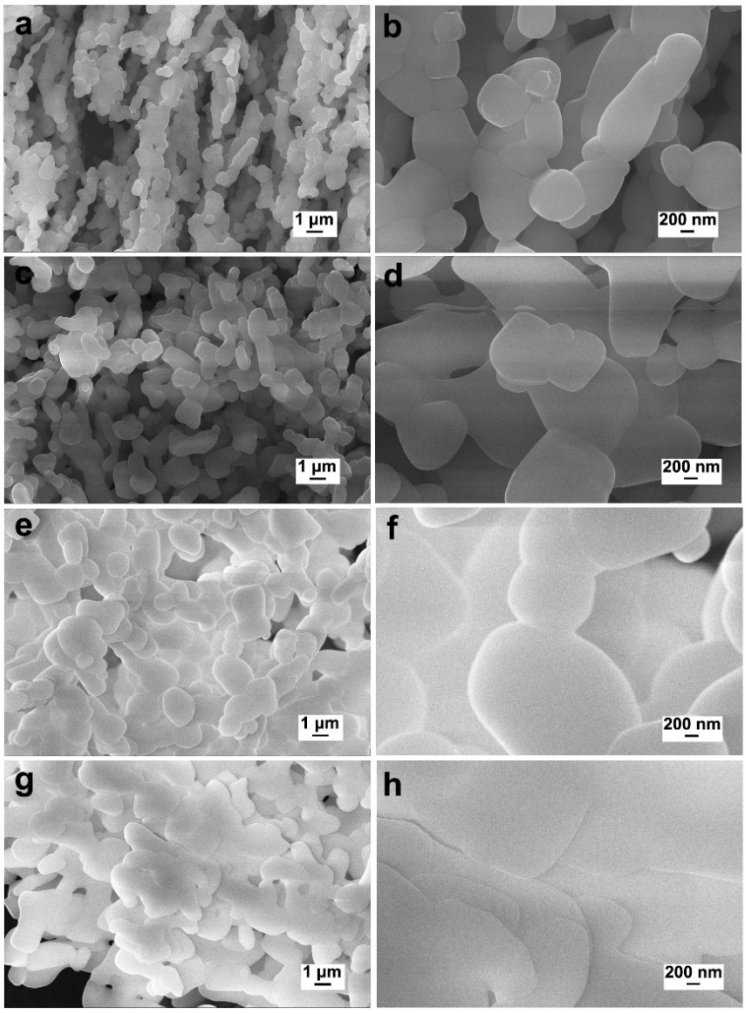

Fig. S5 SEM images of (a,b) NaCl-1, (c,d) NaCl-4, (e,f)NaCl-8 and (g,h) NaCl-16.

Fig. S5 shows the SEM iamges of NaCl scaffolds when NaCl solution was treated with liquid nitrogen without the addition of F127 and rhodanine. (1) With the increasing amount of NaCl, the particle size becomes larger and these particles tend to agglomerate with each other. (2) Without the addition of F127 and rhodanine, the collision of nanocrystals is strong to form nanocrystal agglomeration with large size even at a low amount of NaCl.

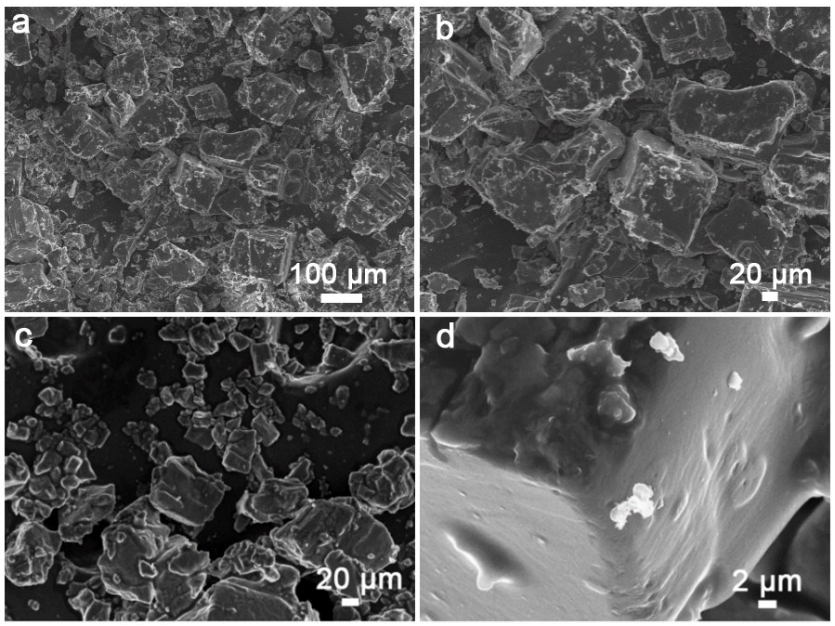

Fig. S6. SEM images of (a,b) pre-RC and (c,d) pre-FC.

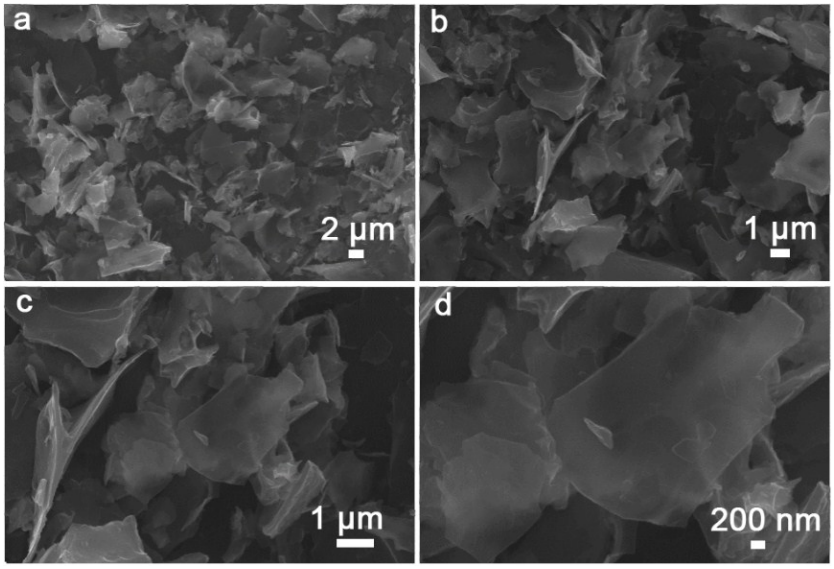

Fig. S7. SEM images of RC.

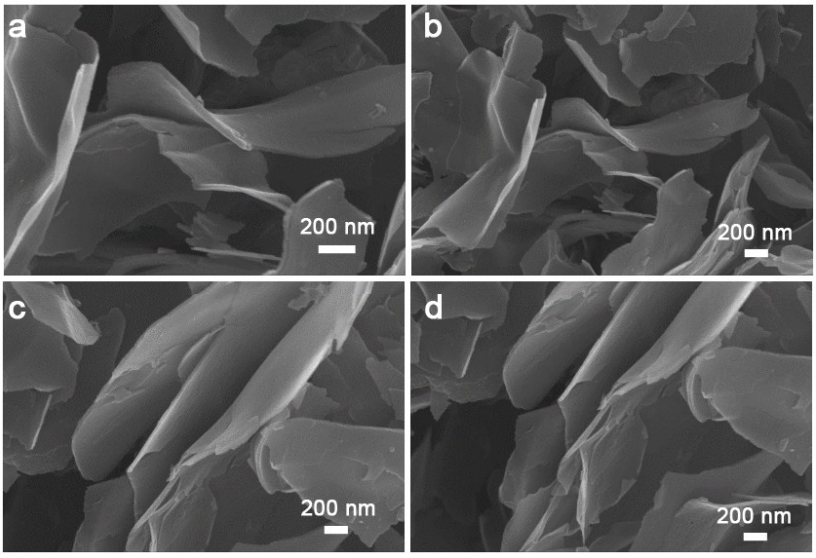

Fig. S8. SEM images of FC.

The salt crystals size of pre-RC (Fig. S6a,b) is much larger than that of pre-FC (Fig. S6c,d). It is because of the strong interactions between inorganic crystals and F127. During drying, F127 would be adsorbed on the surface of NaCl crystals to hinder the growth of NaCl nanocrystals.[1] Furthermore, F127 can better coat the NaCl crystals than rhodanine. So the morphology of FC (Fig. S8) is more uniform than that of RC (Fig. S7), and the thickness of FC is lower.

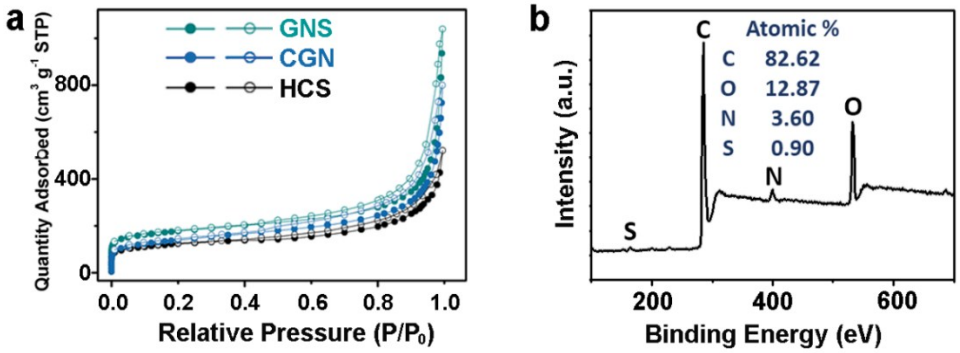

Fig. S9. (a) nitrogen adsorption/desorption isotherms of HCS, CGN and GNS; (b) XPS survey spectrum of CGN.

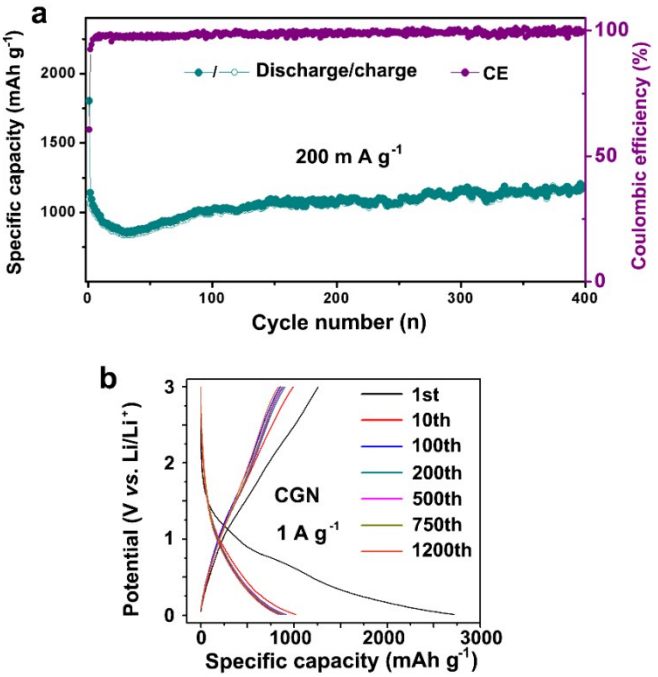

Fig. S10. (a) Long-term cyclic performance of CGN at 0.2 A g^{-1}; (b) voltage profiles of CGN from 1st to 1200th cycle at 1 A g^{-1}.

As shown in Fig. S10a, the reversible specific capacity of CGN maintains 1180 mAh g^{-1} at 200 mA g^{-1} after 400 cycles.

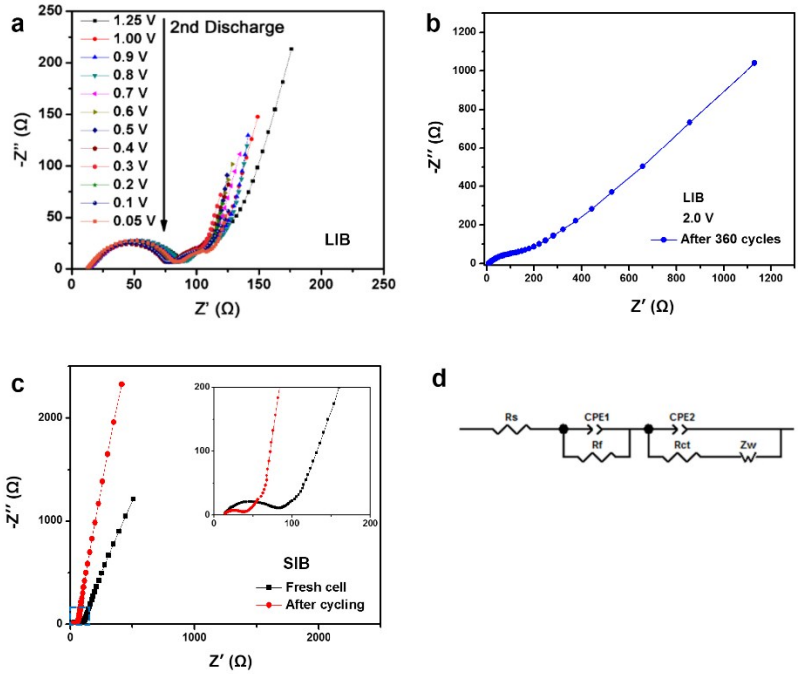

Fig. S11. (a) Nyquist plots of CGN electrode (a) in the 2nd discharge process and (b) after 360 cycles in LIBs; (c) nyquist plots of CGN electrode before and after cycling in SIBs; (d) randles equivalent circuit for the CGN electrodes.

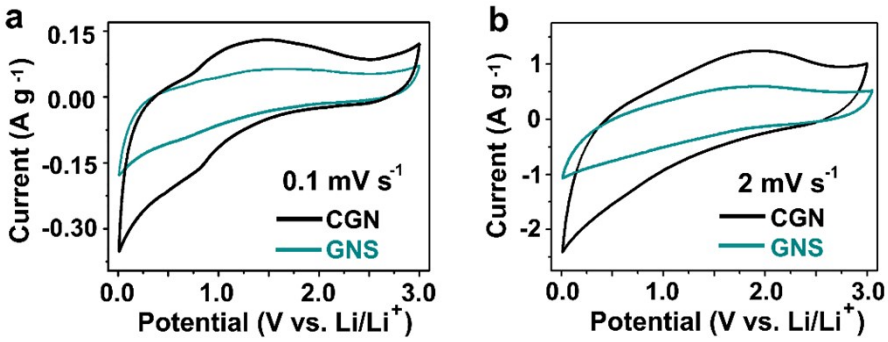

Fig. S12. CV curves of CGN and GNS electrodes at (a) 0.1 and (b) 2 mV s^{-1}

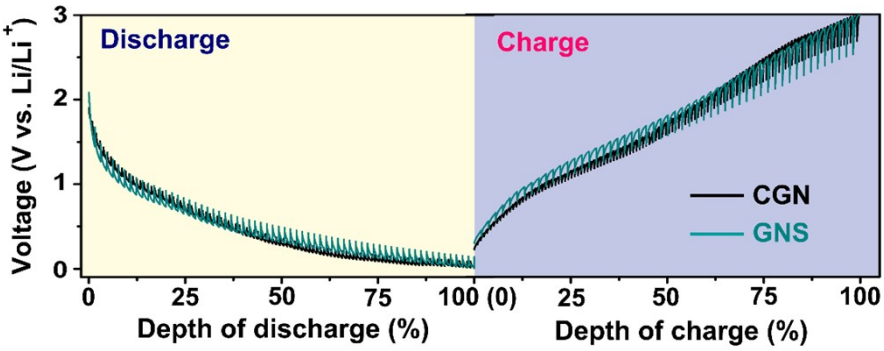

Fig. S13. GITT curves of CGN and GNS electrodes.

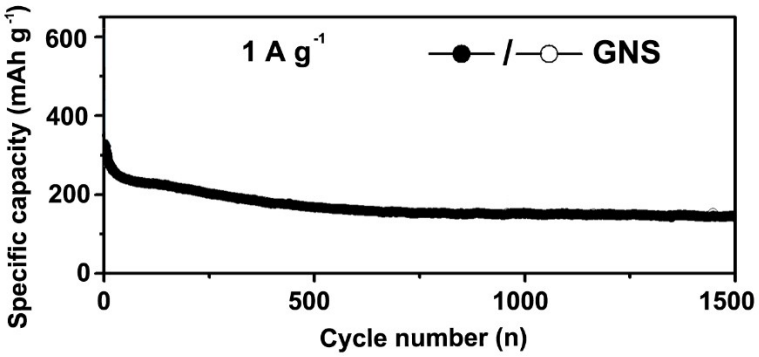

Fig. S14. Long-term cyclic performance of GNS at 1 A g^{-1} as SIB anode materials.

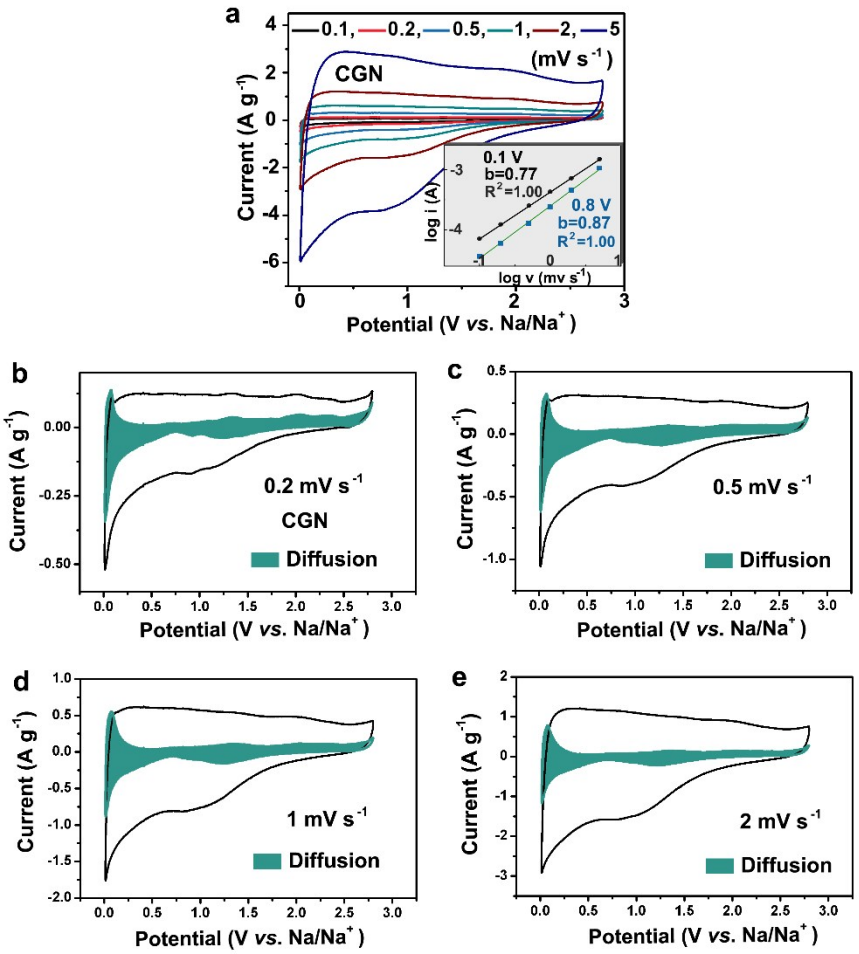

Fig. S15. (a) CV curves of CGN from 0.1 to 5 mV s^{-1}; (b-e) Diffusion contribution ratio of CGN in SIBs at different scan rates

Supplementary Tables

Table S1. Specific surface areas the products calculated by DFT method

Sample	S_{BET} (m^2 g^{-1})	S_{mic} (m^2 g^{-1})	S_{mes} (m^2 g^{-1})
HCS	442.4	143.4	299.0
CGN	576.8	244.6	332.3
GNS	471.8	106.5	365.2

S_{BET}: BET surface area. S_{mic}: t-Plot micropore area. S_{mes}: t-Plot mesopore area.

Calculation of diffusion-controlled and capacitive contribution:

The diffusion-controlled process in CGN and GNS electrodes can be studied by the power law relationship between current *i* and scan rate *v*:[2-4]

$$i = av^b,$$

where i is the current, v is the scan rate, and a and b are adjustable parameters. A *b*-value of 0.5 represents a fully diffusion-controlled process and a *b*-value of 1.0 indicates a capacitive process.

The contribution of these two processes can be separated quantitatively by the following equation:

$$i(v) = k_1 v + k_2 v^{1/2}$$

In this equation, $k_1 v$ represent the capacitive contribution, and $k_2 v^{1/2}$ represents the diffusion-controlled contribution.

And this equation can be rearranged to the equation as follows for easy analysis.

$$i(v) / v^{1/2} = k_1 v^{1/2} + k_2$$

Then k_1 and k_2 can be determined by fitting a straight line of $i(v) / v^{1/2}$ vs. $v^{1/2}$, in which k_1 is the slope and k_2 is the y-intercept.

Calculation of diffusion-contributed capacity and adsorption-contributed capacity:

Trasatti method is used to evaluate the total capacity, diffusion-contributed capacity and adsorption-contributed capacity:[5, 6]

$$C = \frac{1000S}{3.6v\Delta Um}$$

where C (mAh g^{-1}) is the gravimetric capacity, S (mA V) is the quantitative CV integral area of cathode scan, v (mV s^{-1}) is the scan rate, ΔU (V) is the voltage window, and m (mg) is the mass of active materials on a single electrode.

REFERENCES:

1. Y. Chen, L. Shi, Q. Yuan, A. Li, S. Huang, H. Y. Yang, X. Chen, J. Zhou and H. Song, *ACS Nano*, 2018, **12**, 4019-4024.
2. H. Lindstrom, S. Sodergren, A. Solbrand, H. Rensmo, J. Hjelm, A. Hagfeldt and S.-E. Lindquist, *J. Phy. Chem. B*, 1997, **101**, 7717-7722.
3. H. Kim, J. Hong, Y.-U. Park, J. Kim, I. Hwang and K. Kang, *Adv. Funct. Mater.*, 2015, **25**, 534-541.
4. T. Brezesinski, J. Wang, J. Polleux, B. Dunn and S. H. Tolbert, *J. Am. Chem. Soc.*, 2009, **131**, 1802-1809.
5. Y. Dong, S. Zhang, X. Du, S. Hong, S. Zhao, Y. Chen, X. Chen and H. Song, *Adv. Funct. Mater.*, 2019, **29**, 1901127.
6. T. Lin, W. Chen, F. Liu, C. Yang, H. Bi, F. Xu and F. Huang, *Science*, 2015, **350**, 1508-1513.